Depth-Assisted Segmentation for Forest Carbon Inventories

Bill Tong
University of Waterloo
Waterloo, Canada

Amelia Holcomb
University of Waterloo
Waterloo, Canada
aholcomb@uwaterloo.ca

Srinivasan Keshav
Cambridge University
Cambridge, UK
sk818@cam.ac.uk

ABSTRACT

TODO: A clear and well-documented LaTeX document is presented as an article formatted for publication by ACM in a conference proceedings or journal publication. Based on the "acmart" document class, this article presents and explains many of the common variations, as well as many of the formatting elements an author may use in the preparation of the documentation of their work.

CCS CONCEPTS

• **Computer systems organization** → **Embedded systems**; *Redundancy*; Robotics; • **Networks** → Network reliability.

KEYWORDS

datasets, neural networks, gaze detection, text tagging

ACM Reference Format:
Bill Tong, Amelia Holcomb, and Srinivasan Keshav. 2021. Depth-Assisted Segmentation for Forest Carbon Inventories. In *Proceedings of HotMobile '21: Annual International Workshop on Mobile Computing Systems and Applications (HotMobile '21).* ACM, New York, NY, USA, 8 pages.

1 INTRODUCTION

It is by now well-recognized that carbon sequestration in woodlands and forests can play a key role in decarbonizing the atmosphere and averting catastrophic climate change. In its 2018 report, the Intergovernmental Panel on Climate Change (IPCC) highlights that all pathways to limit global warming to 1.5C rely on carbon dioxide removal, with most published plans incorporating forest carbon sequestration specifically [19]. However, strategies to achieve these reforestation goals, whether through policy- or market-based incentives, still face a technological challenge: they require extensive monitoring, reporting, and verification (MRV) tools to evaluate the carbon sequestration achieved [5] [12] [16] .

Current forest MRV uses a well-standardized but highly manual forest inventory process. Foresters measure key features related to carbon sequestration by hand, for example using tape measures or calipers to find the diameter of each tree trunk and mapping out appropriate sample plots with ribbon or rope. The process is expensive, time-consuming, and labor-intensive, which has several important consequences. First, it limits the sample size for forest measurement, both at the individual forest level and across the earth as whole, where only a tiny fraction of forested land has been actively sampled. Second, it limits the number of data points that can be collected per tree, since the process is carried out by hand and data entry is manual. Finally, and most importantly for our research, it falls short of what is needed to rapidly scale up carbon sequestration incentive programs. The resource-intensive process places too heavy a burden on small-scale reforestation efforts. At the same time, reforestation and anti-deforestation efforts in large tropical forests are difficult to measure with these manual methods due to the forests' size and density.

To this end, we see great promise in the rapid increases in technical sophistication of commodity smartphones, which allow them to be used in non-traditional applications. In this paper, we explore the use of new time-of-flight (depth) sensors, now outfitted on flagship phones, to measure trees in realistic forest settings. By improving the ease and efficiency of the forest inventory process, we believe it will be possible to measure tree plots rapidly, accurately, and at low cost.

Although we are not the first to recognize the power of smartphones for forest plot inventories, prior attempts have relied on tree trunks that are well-spaced, brightly lit, and suffer minimal occlusion [10] [11]. In practice – particularly in the natural forest environments that carbon sequestration incentive schemes may hope to foster – these conditions are unlikely to hold. In contrast, we are able to accurately measure tree trunk diameter (or Diameter at Breast Height,

Unpublished working draft. Not for distribution.

Permission to make digital or hard copies of all or part of this work for personal or classroom use is granted without fee provided that copies are not made or distributed for profit or commercial advantage and that copies bear this notice and the full citation on the first page. Copyrights for components of this work owned by others than ACM must be honored. Abstracting with credit is permitted. To copy otherwise, or republish, to post on servers or to redistribute to lists, requires prior specific permission and/or a fee. Request permissions from permissions@acm.org.
HotMobile '21, February 24–26, 2021, Cyberspace
© Association for Computing Machinery.
ACM ISBN 978-x-xxxx-xxxx-x/YY/MM…$15.00

Unpublished working draft. Not for distribution.

DBH) under complex field conditions. Specifically, we make the following contributions:

- We present the design of an algorithm that exploits the time-of-flight sensor on a smartphone to estimate DBH from a single image, even in the face of leaf and branch occlusion.
- We implement this design on a Huawei P30 Pro Smartphone, and demonstrate that it is efficient enough to perform in real-time.
- We evaluate our algorithm in a realistic setting and find that in a corpus of 42 sample tree images, it has a detection rate of 95%, with RMSE of 2.88 cm.

2 BACKGROUND

2.1 Traditional Forest Inventory

Forest surveying is a well-established field, encompassing both managed timber forests and partially managed or unmanaged natural growth forests. The IPCC collected peer-reviewed practices in their Land Use Report [4], offering a global standard for forest carbon measurement that is also followed by the UK's Woodland Carbon Code (WCC) [3]. The land is first divided into homogenous strata, and the strata divided into equally sized plots along a uniform grid. The plots are typically marked out by hand, using a GPS, tape measure, and rope or ribbon, a laborious and time-consuming process.

Tree allometry establishes equations that relate tree biomass to carbon sequestration. These equations generally take as input the tree's diameter at breast height (DBH) and total height, though some use DBH alone. The equations are often specific to a species or other classification of tree (e.g. hardwood, etc.), usually to account for differing wood density. DBH measurements are performed either by measuring tree circumference and dividing by π, or by using specialized calipers that fit around the trunk [20]. Height can be measured with trigonometry using a meterstick, but surveyors often use technical equipment such as a hypsometer. Top-of-the-line all-in-one devices are around $2000 USD, though there are cheaper models for around $387 USD.[1] The appropriate species identification or other classification is done manually by field experts. Further equations relate biomass to an estimate of carbon sequestration.

Though this process is well-established, it has several key limitations. First, it is both time and cost-intensive. Carrying equipment into the forest, marking out plots, and measuring each tree individually all add to the time required. Second, a relatively high level of expertise is required to correctly place sample plot boundaries, measure trees accurately, and identify tree species. The time and expertise both translate to costs that small-scale reforestation efforts may not be able to meet. Finally, the entire process yields only a few data points per tree (such as species, DBH, height, biomass) – and no rich datasets like images that could yield substantial additional information after the surveyors have left the forest.

Indeed, the high barriers to entry also results in a less accurate process overall. The more time, cost, and expertise is required, the less total land can be easily surveyed, meaning surveyors have to rely more heavily on statistical sampling methods to extrapolate sequestration estimates [4]. It also leads to underrepresentation of forests that are dense, diverse, and hard-to-reach, like tropical forests [cite].

Capability	TLS	SfM	Tango	ToF
Real-time feedback	✗	✗	✓	✓
Single image required	✗	✗	✓	✓
Handles occlusion	✓	✓	✗	✓
Portable and Inexpensive	✗	✓	✗	✓

Table 1: Capabilities of Terrestrial Laser Scanning, Structure from Motion, and the Google Tango system proposed in [11], as compared to our work with the ToF sensor. We highlight the capabilities ideal for performing small-scale forest carbon MRV.

2.2 Related Work

Our proposal draws on the related work of several different fields. Within computer vision, the area of depth-assisted segmentation is relatively well-established. The technology has even come to consumer camera apps, with many flagship phones now advertising a "Bokeh effect" mode in which the background of a photo is automatically detected and blurred. On Google's phones, depth is estimated using SfM and stereo vision techniques with multiple rear-facing cameras, though Huawei and Apple devices equipped with a ToF sensor may be using that sensor instead. In June 2020 Google published its long-awaited Depth API as part of ARCore, though it currently only supports depth measurements from SfM. [2] Until very recently, direct developer access to a ToF depth sensor was mostly limited to specialized or purpose-built AR phones, such as Google's Project Tango [**?**]. It is only now that depth sensors for use with AR integration on ordinary phones are becoming more widespread.

Within forestry, there has been some research into using depth sensing technology to assist forest inventories. In Table 1 we highlight the capabilities and limitations of these technological approaches as compared to our work with the ToF sensor, for the purposes of small-scale forest carbon MRV. We describe the technologies in more detail below.

[1] Sample devices can be found at forestrytools.com.au

[2] https://developers.google.com/ar/develop/java/depth/overview

Unpublished working draft. Not for distribution.

Figure 1: *Left,* Figure 8 from Fan et al. [11], which used Project Tango in a managed forest in the suburbs of Beijing, China. *Right,* A sample image from our work in a naturally managed forest in Waterloo, Canada.

In the main, there are two separate trends within the literature. Silviculturists, focused on highly managed forests often for timber and commercial purposes or around urban areas, have begun using mobile phones with depth sensing and AR for forest inventories. These forests tend to have well-spaced trees with only one or two age classes, and weeds and ground cover (especially near the tree base) is removed. Recent work by Fan et al. used Project Tango to estimate DBH, height, and stem position in a commercial forest setting, achieving an RMSE of 1.26cm and bias of 0.33cm for DBH measurements. These works have dramatically simplified the computational problem by studying highly managed forests. In Figure 1, we show an image of the forest environment measured by Fan et al, side-by-side with a typical image from the natural-growth forest used in our research. We can see that the natural-growth forest sees high levels of occlusion and variegated light even across a single tree trunk. This makes segmentation a considerably harder task.

Notably, the limitations of the related research in silvicultural contexts precludes their use in precisely the environments that are of most significance from a climate perspective. The ideal incentive system for carbon sequestration would reward naturally managed forests over highly managed timber forests, since the former is likely to offer additional ecosystem services such as improved biodiversity and increased habitat for native species. Our proposed MRV system prioritizes climate and sustainability, addressing the challenges of natural forests as its primary use-case.

Separately, there is research on new methods in forest ecology, which often targets old-growth forests. The research community here has not extensively pursued mobile AR methods, but has used medium-range LiDAR Terrestrial Laser Scanning (TLS) for forest surveys. Their results have been impressive, speeding up the forest inventory process and leading to direct improvements in allometric equations for biomass estimation [21] [15] [8].

However, TLS instruments have direct trade-offs between signal noise and range and sensor cost. One detailed forest study, published in 2018 but with field work done in 2015, used LiDAR costing 75K-150K GBP per instrument [9]. The authors mention that their instruments are at the upper range of TLS scanner cost, with a range of 700m and a pointing accuracy of millimeters at that range. Several authors mention that TLS scanners *can* cost closer to the 10K range, but their research actually uses an instrument costing over 50K [9] [23]. Wilkes et al. note that instrument weight can also be an issue, given that many sensors are over 10kg and "can be heavy and awkward to carry through dense vegetation" [23]. These instruments seem suitable for well-funded research groups, but have not been adopted in government MRV programs.

Other research in forest ecology has highlighted the need for a more affordable, portable, and technologically accessible approach to forest surveying [13] [18]. Piermattei et al. write,

> "Currently, terrestrial laser scanning (TLS) is the remote sensing method that provides the most accurate point clouds at the plot-level to derive [tree attributes] from. However, the demand for even more efficient and effective solutions triggers further developments to lower the acquisition time, costs, and the expertise needed to acquire and process 3D point clouds, while maintaining the quality of extracted tree parameters." [18]

These researchers have experimented with Structure from Motion (SfM) on mobile platforms, obtaining point clouds as

Unpublished working draft. Not for distribution.

a user moves through the forest. Within forest ecology, work on terrestrial SfM is still in an immature stage of development relative to TLS. It typically focuses on measurement of single trees and does not extend them to a full plot context, with the work by Piermattei et al. being a notable exception. Their work captures images with a Nikon digital SLR camera and performs offline processing with PhotoScan Pro to derive dense point clouds. Our research proposes an alternative to SfM that can offer the same benefits of decreased cost and expertise barriers, while potentially improving accuracy and lowering acquisition time and processing power. Indeed, with ToF scanning and the software available on new mobile phones, we may be able to perform a significant amount of the processing on the phone itself, providing the opportunity for users to correct and adjust easily while still on-site. Moreover, the proposal outlined here requires only a single photograph per tree to accurately estimate DBH, while Piermattei et al. require numerous photographs both to perform SfM and to handle occlusion.

2.3 Segmentation in Forest TLS and SfM

In highly automated forest inventory systems such as TLS, segmentation is a key issue. Research focuses on both distinguishing leaves from branches and distinguishing trees from other trees. Some researchers use specialized dual-wavelength LiDAR to separate leaves from branches [14]; others complete TLS inventories in leaf-off conditions, partly to simplify the segmentation problem [21]. Of course, relying on leaf-off conditions is not always possible, and limits inventories to deciduous forests. One software package used for segmentation in forest TLS is treeseg, developed by Burt et al. [7]. This software is run offline, after data collection, and separates trees by looking for neighborhoods of the point cloud that share similar surface normal vectors (which are therefore likely to belong to the same surface).

Many terrestrial SfM studies sidestep the issue of segmentation, usually by examining only single trees rather than full plots – thus assuming from the start that the tree in question is represented by the studied point cloud [13] [17]. Bauwens et al. clear nearby vegetation by hand, and use a significant amount of manual data processing [6]. The only SfM study to our knowledge that handles segmentation is from Piermattei et al., which makes use of the Forest Analysis and Inventory Tool, FAIT. FAIT is an offline point cloud processing tool that finds tree stems by looking for long linear clusters [18].

3 DESIGN AND IMPLEMENTATION

3.1 Mobile Phone Hardware and Software

In our research, we used a Huawei P30 Pro phone, which retails for around $1000 USD. It has three rear-facing cameras (40, 20, and 8 MP), one rear-facing TOF sensor, and a front-facing camera (32 MP). It is also equipped with 128GB of SSD storage, 6GB of RAM, an Octa-core CPU and a separate GPU. For full technical specifications, see Appendix **??**. The Huawei P30 Pro is a flagship smartphone, but it is not purpose-built for AR tasks. Of the smartphones with a ToF sensor, Huawei's offered the most adaptable APIs with direct access to raw sensor data through both the Android Camera2 API[1] and the Huawei AREngine API [2]. Samsung, the chief competitor producing Android phones with a ToF sensor, only allowed ToF use through existing Samsung apps at the time, though it now offers similar flexibility.

Initially, we accessed the raw ToF sensor data directly through the android.hardware.camera2 API. This is workable for depth data alone, but does not (as of writing) provide sufficient support to programmatically combine depth and RGB camera information into a single image. The first challenge is issuing two simultaneous (or near-simultaneous) capture requests to each camera. Android offers a multicamera API, with which multiple physical cameras that face the same direction can be combined into a single logical camera at the software layer, with capture requests dispatched to each. However, this API does not seem to officially support combining a depth camera with an RGB camera. [3] Indeed, when we attempted it, the ToF sensor results no longer corresponded to correct depths, though whether this is an API problem or a hardware problem is unclear. Second, the calibration matrices for the ToF and RGB cameras, supposed to be programmatically accessible with the LENS_INTRINSIC_CALIBRATION camera characteristic, were not populated by Huawei in the camera2 Java API. Moreover, the physical translation between the two sensors was not exposed in any place that we were able to find. This made programmatic overlay of RGB and depth images impossible without physical camera calibration.

Instead, we used the Huawei AR Engine SDK.[4] The Huawei ARFrame object has functions `acquireCameraImage()` and `acquireDepthImage()`, which allow working with the RGB and ToF cameras simultaneously. The Huawei depth data retrieved through this API is pre-calibrated with the RGB image, so the two can be rescaled to the same height and width and then overlaid. See section 3.2 for more details on this process.

3.2 Post-Processing Software

3.2.1 RGB+D Images. The first step in post-processing is to combine the RGB and Depth images into a single RGB+D

[3] An Android development guide states, "We can expect that, in most cases, new devices launching with Android Pie will expose all physical cameras (the exception being more exotic sensor types such as infrared) along with an easier to use logical camera." [22]

[4] It is perhaps worth noting that the API documentation for this SDK, as of writing, only exists in Chinese.

Unpublished working draft. Not for distribution.

image format. As mentioned above, the Huawei ARFrame API pre-calibrates the RGB and Depth images, so no transformations are required based on the intrinsic parameters of the two sensors, nor the rotation and translation between the two.

Only two adjustments are required. First, Huawei returns the depth data as a buffer of `unsigned shorts` in DEPTH16 format. This works well in C++, but the Huawei API does not accommodate for the fact that in Java the endianness is reversed. The two bytes representing each depth pixel must therefore be reversed before they can be parsed as DEPTH16.

Second, the depth data is at resolution 240 x 180, while the RGB image has resolution 640 x 480. Instead of downsampling the RGB image, which loses a significant amount of data, we upsampled the depth data using the Kronecker product. [Include formula]

3.2.2 Trunk Segmentation. Given the RGB-D image, the next step is to segment the tree trunk from the rest of the image, the primary challenge here being the typical level of occlusion and light variegation in a natural forest context under leaf-on conditions. [Figure].

To label the tree trunk pixels in the image, we took the following approach:

(1) Find an approximate depth value associated with the tree trunk.
(2) Filter the RGB+D image for pixels whose depth value is within a small range of the trunk depth.
(3) Fit the filtered pixels in order to remove outliers and fill in areas of the trunk that were missing due to obstruction.

To find the approximate depth value of the tree trunk, we began with the natural assumption that the photographer would attempt to roughly center the tree trunk in the image. We sliced the image vertically into thirds, and took the modal depth value from the center third of the image as the approximate trunk depth. Next, we filtered the entire image for pixels whose depth value is within ±10% of the approximate trunk depth. This forms a rough segmentation.

This segmentation tended to include some outlier leaves and branches that happened to match the trunk depth, while omitting portions of the trunk that were obscured by closer leaves and branches. It was not yet sufficient to provide an accurate trunk diameter estimate.

Initially, we attempted to use the QHull algorithm to find a convex hull for the pixels remaining in the center third of the image. This simple approach easily fills in the missing portions of the trunk obscured through occlusion, but is overly sensitive to small protrusions around the edge of the trunk, for example the beginning of lower branches. Instead, we used stricter assumptions about the trunk shape by fitting linear boundaries to its edges.

Since the remaining pixels post-filtering are dominated by trunk pixels, they form an oblong cluster with outliers. We find the principal axis of the trunk using Principal Component Analysis, and rotate the image back by the angle of this axis so that the trunk is vertical. With the rotated image, we search iteratively inward along vertical scanlines from the left and right border for the first scanline at which more pixels are in the cluster than not. This forms the left and right boundary of the trunk. The final segmentation consists of all the cluster pixels that lie within this boundary.

3.2.3 Diameter Estimation. **TODO: Describe translation from pixels to widths**

TODO: Calculate appropriate bias correction and describe

4 EVALUATION

We evaluated our work in the Laurel Creek and Avon forests of Waterloo, Canada. The former is part of a larger nature preserve, and both are naturally managed forests including multiple northern tree species and age classes. We measured during midsummer leaf-on conditions, resulting in natural trunk occlusion from leaves and branches across the samples.

In total, we took 42 samples of 26 trees, with an image of each tree taken at 1m and 2m away. All of the samples were taken on a Huawei P30 Pro phone running our app, and each image was then processed separately to estimate the tree's DBH. We used a tape measure to compute the reference DBH to the nearest centimeter, and found that the samples ranged in diameter between 8-33cm. We compared our results with the work of Fan et al. and Piermattei et al., who attempt to measure DBH with Google Tango and Structure from Motion, respectively. Piermattei et al. also compare their results with TLS used over the same plots, so we include their TLS results in Table 2, comparing the bias and RMSE of each method over its evaluation sample.

In two of our 42 samples, the camera was unable to obtain any depth points for the tree. We omitted these samples from our error evaluation, below, and recorded our detection rate in the sample as 95%. See section 5.1 for further discussion of trunk detection. Omitting these two samples, figure 2 shows the distribution of errors across our dataset. The RMSE was XX, with bias XX. Table 2 compares these values to the overall RMSE and bias for SfM, TLS, and Google Tango, as reported by Piermattei and Fan. 2cm of error is considered sufficient accuracy for field inventory DBH measurements [18].

[We note that these results are not entirely comparable because they were obtained from different samples. We compared images from the papers of Piermattei and Fan to our own forest plots, and found that Fan in particular used a forest setting which appears to have little to no occlusion (see

Unpublished working draft. Not for distribution.

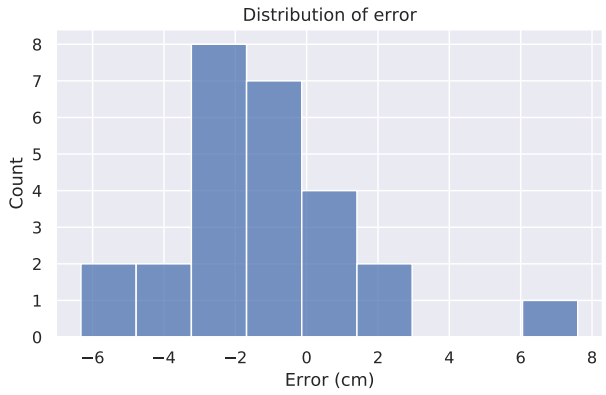

Figure 2: Distribution of errors for our 42-image sample.

	TLS	SfM	Tango	ToF
Bias (cm)	-0.77	-1.13	0.33	-1.26
RMSE (cm)	2.43	3.40	1.26	2.88

Table 2: Comparison of Bias and RMSE across various studies and methods. TLS and SfM were evaluated by Piermattei et al. in [18] (they report separate statistics per plot, so the results are aggregated across all four plots); Google Tango was evaluated by Fan et al in [11]; ToF was evaluated in this work.

figure 1). We note that Fan reports smaller error and bias than TLS, which is surprising enough to suggest that the authors did not choose an evaluation environment representative of the challenges of a typical natural forest. For comparison, we split our sample into "occluded" and "unoccluded" and compared our work with theirs on the unoccluded images. **TODO: Do this.**]

We also examined our error with respect to tree diameter. While Piermattei et al. found no significant effect of tree diameter on error, with a Wilcoxon Rank Test showing the effect is insignificant ($p >> 0.05$). Fan et al. find that their system tends to underestimate tree diameter more as DBH increases, and we see a similar effect in Figure 3.

Finally, we considered whether the distance at which the image was taken (1m or 2m) had an effect on the error. The side-by-side boxplots can be seen in Figure 4, along with their means and variance. We ran a Wilcoxon rank test on the paired samples (dropping the two trees with 8cm diameter altogether, since their pairs at 2m were undetected) and it did not find a significant effect, but given the small sample size and the effect of removing both samples with small diameter, it seems prudent to ignore the test and consider Figure 4

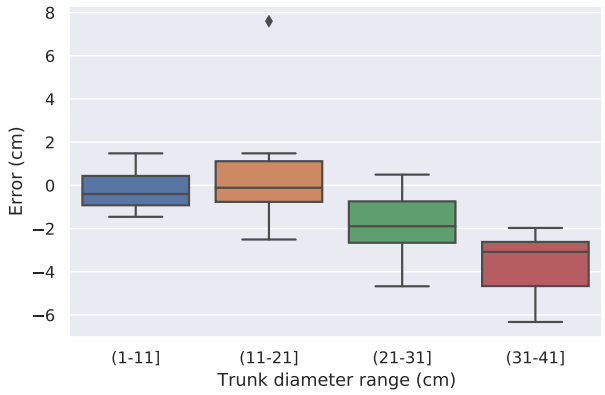

Figure 3: Trunk diameter vs error. Note that the first bucket has overly low error and variance, because it would contain two samples with 8cm diameter at 2m away, but they were dropped because the trunk was undetected.

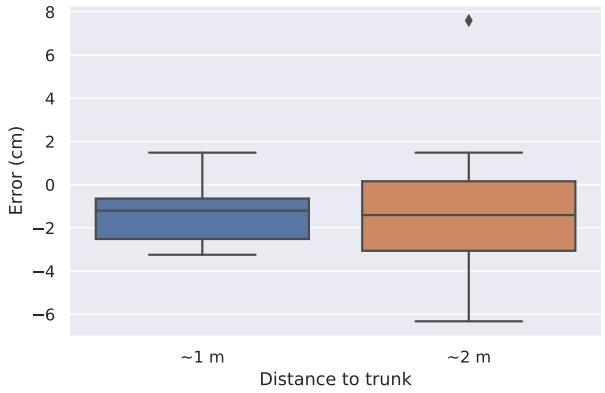

Figure 4: DBH error distribution for trees at approximately 1m and 2m away. At 1m away, the samples had mean error -1.35 and error variance of 0.02. At 2m away, the samples had mean error -1.16 and error variance 0.13.

more qualitatively. The mean error (bias) is similar at both distances, and the variance of the error is only slightly larger at 2m, though further data is required to confirm this. It seems that there is not much difference in cases where the tree is detected at all, but thinner trees are more likely to go entirely undetected at 2m.

Unpublished working draft. Not for distribution.

5 DISCUSSION

5.1 Detection

In two of our 42 samples, the camera was unable to obtain any depth points for the tree. Both of these images were taken at 2m away, and the reference trunk diameter was 8 cm. These were the only two trees with diameter under 10 cm in the sample, and their trunk diameter was measured accurately at 1m away. Piermattei et al. found that using SfM, the average diameter of undetected trees in their sample was 12cm. Fan et al. did not report any trees undetected, however they also did not specify the process by which they took images, nor the distance they stood from the tree.

At the time we performed our evaluation, the app provided no user feedback – the user could not even view captured RGB-D images to see that no depth points were registered until after the images were uploaded and processed. This created an ideal blind experiment setting, examining the power of the ToF sensor and our algorithm without any user assistance. However, part of the strength of the ToF sensor and mobile phone application is the simplicity of the algorithms required to process the data and the ease of real-time computation and feedback (see section 5.2). If a user tapped the screen to indicate they expected a tree trunk to be in view, but no depth points were currently registered, the app could, in real time, ask the user to step closer to the tree.

5.2 Processing time

Though we developed our trunk segmentation and diameter estimation to run as an offline processing pipeline, ultimately the algorithms used were not CPU-intensive and could certainly be run in real-time on the mobile phone. We are currently working to port them back into our RGB-D app. This would be a notable improvement over existing SfM and TLS systems, because it would enable real-time feedback about the success or failure of data collection. For comparison, Piermattei et al. require 17-52 hours of post-processing time for SfM to co-register and orient images before they can begin identifying and measuring tree trunks. This precludes the possibility of providing real-time feedback in the field. While Piermattei et al. find TLS takes only three hours of post-processing time, this is still too long to provide automatic assistance during data collection.

5.3 Future Work

TODO: Discuss future work

6 CONCLUSION

TODO: Lorem ipsum dolor sit amet, consectetuer adipiscing elit. Etiam lobortis facilisis sem. Nullam nec mi et neque pharetra sollicitudin. Praesent imperdiet mi nec ante. Donec ullamcorper, felis non sodales commodo, lectus velit ultrices augue, a dignissim nibh lectus placerat pede. Vivamus nunc nunc, molestie ut, ultricies vel, semper in, velit. Ut porttitor. Praesent in sapien. Lorem ipsum dolor sit amet, consectetuer adipiscing elit. Duis fringilla tristique neque. Sed interdum libero ut metus. Pellentesque placerat. Nam rutrum augue a leo. Morbi sed elit sit amet ante lobortis sollicitudin. Praesent blandit blandit mauris. Praesent lectus tellus, aliquet aliquam, luctus a, egestas a, turpis. Mauris lacinia lorem sit amet ipsum. Nunc quis urna dictum turpis accumsan semper.

ACKNOWLEDGMENTS

TODO: Identification of funding sources and other support, and thanks to individuals and groups that assisted in the research and the preparation of the work should be included in an acknowledgment section, which is placed just before the reference section in your document.

REFERENCES

[1] [n.d.]. android.hardware.camera2. https://developer.android.com/reference/android/hardware/camera2/package-summary

[2] [n.d.]. HUAWEI AR Engine - HMS Core - HUAWEI Developer. https://developer.huawei.com/consumer/en/hms/huawei-arengine/

[3] [n.d.]. The Woodland Carbon Code scheme for buyers and landowners. https://www.gov.uk/guidance/the-woodland-carbon-code-scheme-for-buyers-and-landowners

[4] 2003. *Good Practice Guidance for Land Use, Land-Use Change and Forestry.* Technical Report. Intergovernmental Panel on Climate Change. https://www.ipcc-nggip.iges.or.jp/public/gpglulucf/gpglulucf_files/Chp4/Chp4_3_Projects.pdf

[5] 2020. *Land use: Policies for a Net Zero UK.* Technical Report. Committee on Climate Change. https://www.theccc.org.uk/publication/land-use-policies-for-a-net-zero-uk/

[6] Sébastien Bauwens, Adeline Fayolle, Sylvie Gourlet-Fleury, Leopold Mianda Ndjele, Coralie Mengal, and Philippe Lejeune. 2017. Terrestrial photogrammetry: a non-destructive method for modelling irregularly shaped tropical tree trunks. *Methods in Ecology and Evolution* 8, 4 (2017), 460–471. https://doi.org/10.1111/2041-210X.12670 _eprint: https://besjournals.onlinelibrary.wiley.com/doi/pdf/10.1111/2041-210X.12670.

[7] Andrew Burt, Mathias Disney, and Kim Calders. 2019. Extracting individual trees from lidar point clouds using treeseg. *Methods in Ecology and Evolution* 10, 3 (2019), 438–445. https://doi.org/10.1111/2041-210X.13121 _eprint: https://besjournals.onlinelibrary.wiley.com/doi/pdf/10.1111/2041-210X.13121.

[8] Mathias Disney. 2019. Terrestrial LiDAR: a three-dimensional revolution in how we look at trees. *New Phytologist* 222, 4 (2019), 1736–1741. https://doi.org/10.1111/nph.15517 _eprint: https://nph.onlinelibrary.wiley.com/doi/pdf/10.1111/nph.15517.

[9] M. Disney, Matheus Boni Vicari, A. Burt, Kim Calders, S. Lewis, Pasi Raumonen, and Phil Wilkes. 2018. Weighing trees with lasers: Advances, challenges and opportunities. *Interface Focus* 8 (April 2018),

Unpublished working draft. Not for distribution.

20170048. https://doi.org/10.1098/rsfs.2017.0048

[10] Guangpeng Fan, Feixiang Chen, Yan Li, Binbin Liu, and Xu Fan. 2019. Development and Testing of a New Ground Measurement Tool to Assist in Forest GIS Surveys. *Forests* 10, 8 (Aug. 2019), 643. https://doi.org/10.3390/f10080643

[11] Yongxiang Fan, Zhongke Feng, Abdul Mannan, Tauheed Ullah Khan, Chaoyong Shen, and Sajjad Saeed. 2018. Estimating Tree Position, Diameter at Breast Height, and Tree Height in Real-Time Using a Mobile Phone with RGB-D SLAM. *Remote Sensing* 10, 11 (Nov. 2018), 1845. https://doi.org/10.3390/rs10111845

[12] Julia Grimault, Valentin Bellassen, and Igor Shishlov. 2018. *Key elements and challenges in monitoring, certifying and financing forestry carbon projects.* Technical Report 58. Institute for Climate Economics (I4CE), Paris. https://www.i4ce.org/wp-core/wp-content/uploads/2018/11/1106-i4ce2934-PC58-VA.pdf

[13] Jakob Iglhaut, Carlos Cabo, Stefano Puliti, Livia Piermattei, James O'Connor, and Jacqueline Rosette. 2019. Structure from Motion Photogrammetry in Forestry: a Review. *Current Forestry Reports* 5, 3 (Sept. 2019), 155–168. https://doi.org/10.1007/s40725-019-00094-3

[14] Zhan Li, Alan Strahler, Crystal Schaaf, David Jupp, Michael Schaefer, and Pontus Olofsson. 2018. Seasonal change of leaf and woody area profiles in a midlatitude deciduous forest canopy from classified dual-wavelength terrestrial lidar point clouds. *Agricultural and Forest Meteorology* 262 (Nov. 2018), 279–297. https://doi.org/10.1016/j.agrformet.2018.07.014

[15] Xinlian Liang, Ville Kankare, Juha Hyyppä, Yunsheng Wang, Antero Kukko, Henrik Haggrén, Xiaowei Yu, Harri Kaartinen, Anttoni Jaakkola, Fengying Guan, Markus Holopainen, and Mikko Vastaranta. 2016. Terrestrial laser scanning in forest inventories. *ISPRS Journal of Photogrammetry and Remote Sensing* 115 (May 2016), 63–77. https://doi.org/10.1016/j.isprsjprs.2016.01.006

[16] Richard S Mbatu. 2016. REDD+ research: Reviewing the literature, limitations and ways forward. *Forest Policy and Economics* 73 (Dec. 2016), 140–152. https://doi.org/10.1016/j.forpol.2016.09.010

[17] Martin Mokroš, Jozef Výbošťok, Julián Tomaštík, Alžbeta Grznárová, Peter Valent, Martin Slavík, and Ján Merganič. 2018. High Precision Individual Tree Diameter and Perimeter Estimation from Close-Range Photogrammetry. *Forests* 9, 11 (Nov. 2018), 696. https://doi.org/10.3390/f9110696 Number: 11 Publisher: Multidisciplinary Digital Publishing Institute.

[18] Livia Piermattei, Wilfried Karel, Di Wang, Martin Wieser, Martin Mokroš, Peter Surový, Milan Koreň, Julián Tomaštík, Norbert Pfeifer, and Markus Hollaus. 2019. Terrestrial Structure from Motion Photogrammetry for Deriving Forest Inventory Data. *Remote Sensing* 11, 8 (Jan. 2019), 950. https://doi.org/10.3390/rs11080950 Number: 8 Publisher: Multidisciplinary Digital Publishing Institute.

[19] Joeri Rogelj, Drew Shindell, Kejun Jiang, Solomone Fifita, Piers Forster, Veronika Ginzburg, Collins Handa, Shigeki Kobayashi, Elmar Kriegler, Luis Mundaca, Roland Séférian, Maria Virginia Vilariño, Katherine Calvin, Johannes Emmerling, Sabine Fuss, Nathan Gillett, Chenmin He, Edgar Hertwich, Lena Höglund-Isaksson, Daniel Huppmann, Gunnar Luderer, David L McCollum, Malte Meinshausen, Richard Millar, Alexander Popp, Pallav Purohit, Keywan Riahi, Aurélien Ribes, Harry Saunders, Christina Schädel, Pete Smith, Evelina Trutnevyte, Yang Xiu, Wenji Zhou, Kirsten Zickfeld, Greg Flato, Jan Fuglestvedt, Rachid Mrabet, and Roberto Schaeffer. 2018. *Mitigation Pathways Compatible with 1.5°C in the Context of Sustainable Development.* Technical Report. 82 pages.

[20] Bastienne Schlegel, Jorge Gayoso, and Javier Guerra. 2001. *Manual de Procedimentos para Inventarios de Carbono en Ecosistemas Forestales.* Technical Report D98I1076.

[21] Atticus E. L. Stovall, Anthony G. Vorster, Ryan S. Anderson, Paul H. Evangelista, and Herman H. Shugart. 2017. Non-destructive aboveground biomass estimation of coniferous trees using terrestrial LiDAR. *Remote Sensing of Environment* 200 (Oct. 2017), 31–42. https://doi.org/10.1016/j.rse.2017.08.013

[22] Oscar Wahltinez. 2018. Getting the Most from the New Multi-Camera API. https://medium.com/androiddevelopers/getting-the-most-from-the-new-multi-camera-api-5155fb3d77d9

[23] Phil Wilkes, Alvaro Lau, Mathias Disney, Kim Calders, Andrew Burt, Jose Gonzalez de Tanago, Harm Bartholomeus, Benjamin Brede, and Martin Herold. 2017. Data acquisition considerations for Terrestrial Laser Scanning of forest plots. *Remote Sensing of Environment* 196 (July 2017), 140–153. https://doi.org/10.1016/j.rse.2017.04.030

Unpublished working draft. Not for distribution.